

Method for Microfluidic Whole-Chip Temperature Measurement Using Thin-Film Poly(dimethylsiloxane)/Rhodamine B

Razim Samy, Tomasz Glowdel, and Carolyn L. Ren*

Department of Mechanical and Mechatronics Engineering, University of Waterloo, 200 University Avenue West, Waterloo, Ontario, Canada, N2L 3G1

A novel method is presented for on-chip temperature measurements using a poly(dimethylsiloxane) (PDMS) thin film dissolved with Rhodamine B dye. This thin film is sandwiched between two glass substrates (one of which is 150 μm thick) and bonded to a microchannel molded in a PDMS substrate. Whole-chip (liquid and substrate) temperature measurements can be obtained via fluorescent intensity visualization. For verification purposes, the thin film was tested with a tapered microchannel subjected to Joule heating, with resulting axial temperature gradients comparing well with numerical simulations. Errors induced by the definite film thickness are discussed and accounted for during experimental and analytical analysis. Alternative validation using the traditional in-channel Rhodamine B injection method was also attempted. The thin film has several advantages over traditional methods. First, false intensity readings due to adsorption and absorption of Rhodamine B into PDMS channels are eliminated. Second, whole-chip temperature measurements are possible. Third, separation of working liquid from Rhodamine B dye prevents possible electrophoresis effects.

Recent developments in microfluidic and lab-on-a-chip devices has drawn ever-increasing attention from industrial and academic communities due to their far-reaching applications in chemical, biomedical, environmental, and food processing technologies. Such miniaturized devices generally consist of a glass or plastic microfluidic platform with integrated sample processing units such as mixers, dispensers, reactors, separators, and detection systems for performing chemical and biological assays. Advantages of microfluidic devices over traditional methods include reduced sample and reagent use, increased parallel processing capabilities, and portability. In recent times, there has been a general shift to polymer-based materials such as poly(dimethylsiloxane) (PDMS), due to rapid and low-cost fabrication via soft lithography techniques compared to traditional glass-based devices.^{1–7} In order to effectively design and control microfluidic devices, fluid flow,

heat, and mass transfer must be well understood. For example, a continuous flow microfluidic chip for polymerase chain reaction⁸ requires DNA sample mixtures to be repeatedly pumped through three different temperature regions (i.e., 95 °C for denaturing DNA samples, 72 °C for annealing, and 60 °C for extension). The effective control of temperature is essential for DNA replication and overall chip performance. Heat-transfer control is especially important in analysis techniques such as isoelectric focusing (IEF) with thermally generated pH gradients^{9–11} and temperature gradient focusing.^{12,13} Thus, a reliable on-chip temperature measurement method is required for their development.

There are several commonly used temperature measurement methods in microfluidics. Traditional embedded thermocouples have been adapted for microfluidic applications; however, measurements are limited to single locations unless complex fabrication and data acquisition is implemented for multiple thermocouples.^{14,15} On-chip micromachined sensor arrays made in glass¹⁶ and nuclear magnetic resonance¹⁷ have also been employed providing noninvasive temperature measurement abilities yet suffer from high equipment costs, complex fabrication processes, and implementation difficulties. One of the most popular in situ detection techniques involves the use of Rhodamine B dye, whose fluorescent intensity is strongly temperature dependent.¹⁸ In this method, Rhodamine B is added to the working fluid and the temperature field is determined by monitoring the fluorescent

* To whom correspondence should be addressed. Tel: 519-888-4567 x 33030, Fax: 519-885-5862, E-mail: c3ren@mecheng1.uwaterloo.ca.

(1) Xia, Y.; Whitesides, G. M. *Annu. Rev. Mater. Sci.* **1998**, *28*, 153–184.
(2) Anderson, J. R.; Chiu, D. T.; Jackman, R. J.; Cherniavskaya, O.; McDonald, J. C.; Wu, H.; Whitesides, S. H.; Whitesides, G. M. *Anal. Chem.* **2000**, *72*, 3158–3164.

(3) McDonald, J. C.; Duffy, D. C.; Anderson, J. R.; Chiu, D. T.; Wu, H.; Schueller, O. J. A.; Whitesides, G. M. *Electrophoresis* **2000**, *21*, 27–40.
(4) Ng, J. M. K.; Gitlin, I.; Stroock, A. D.; Whitesides, G. M. *Electrophoresis* **2002**, *23*, 3461–3473.
(5) McDonald, J. C.; Whitesides, G. M. *Acc. Chem. Res.* **2002**, *35*, 491–499.
(6) Chen, X.; Wu, H.; Mao, C.; Whitesides, G. M. *Anal. Chem.* **2002**, *74*, 1772–1778.
(7) Odom, T. W.; Thalladi, V. R.; Love, J. C.; Whitesides, G. M. *J. Am. Chem. Soc.* **2002**, *124*, 12112–12113.
(8) Kopp, M. U.; Mello, A. J.; Manz, A. *Science* **1998**, *280*, 1046–1048.
(9) Slais, K. *J. Chromatogr., A* **1996**, *730*, 247–259.
(10) Fang, X. H.; Adams, M.; Pawliszyn, J. *Analyst* **1999**, *124*, 335–341.
(11) Huang, T.; Pawliszyn, J. *Electrophoresis* **2002**, *23*, 3504–3510.
(12) Ross, D.; Locascio, L. E. *Anal. Chem.* **2002**, *74*, 2556–2564.
(13) Kim, S. M.; Sommer, G. J.; Burns, M. A.; Hasselbrink, E. F. *Anal. Chem.* **2006**, *78*, 8028–8035.
(14) Khandurina, J.; Mcknight, T. E.; Jacobson, S. C.; Waters, L. C.; Foote, R. S.; Ramsey, J. M. *Anal. Chem.* **2000**, *72*, 2995–3000.
(15) Lagally, E. T.; Medintz, I.; Mathies, R. A. *Anal. Chem.* **2001**, *73*, 565–570.
(16) Xue, Z.; Qiu, H. *Sens. Actuators, A* **2005**, *112*, 189–195.
(17) Lacey, M. E.; Webb, A. G.; Sweedler, J. V. *Anal. Chem.* **2000**, *72*, 4991–4998.
(18) Ross, D.; Gaitan, M.; Locascio, L. E. *Anal. Chem.* **2001**, *73*, 4117–4123.

intensity using microscopy techniques. Due to its excellent spatial and temporal resolution, Rhodamine B has been used extensively to study Joule heating and heat-transfer effects in glass and PDMS-based microfluidic chips.^{19–21} Although Rhodamine B temperature measurements have been somewhat successful, three major issues exist as discussed below.

Absorption of Rhodamine B into PDMS Chips. Recently it has been discovered that compatibility issues exist for polymer-based microfluidic chips and neutral hydrophobic fluorescent dyes commonly used for temperature and flow visualizations.^{22,24} In the case of Rhodamine B, the dye will adsorb and diffuse into the PDMS material. Fluorescent images of a PDMS channel (150 μm wide and 100 μm high) after 10, 20, and 30 min of the introduction of Rhodamine B (Fisher Scientific, Ottawa, Canada) (100 μM in deionized water) are shown in Figure 1. Large amounts of Rhodamine B initially in the fluid have absorbed into the surrounding PDMS. In addition, adsorption occurs in the gathering of dye particles at the solid–liquid interface resulting in a stacking effect that creates intensity peaks at the wall as shown in Figure 1. Although the dye diffuses into the PDMS, overall concentration in the fluid does not decrease due to continuous replenishment from the reservoirs. On the contrary, overall fluorescent intensity increases with time due to Rhodamine B diffusion into the top PDMS channel surface resulting in an artificial change in temperature.²¹ The adsorption also alters the ζ potential and consequentially the electroosmotic flow in the microchannel.²²

Other researchers have attempted to solve this problem by modifying the surface properties of PDMS. Roman et al. were successful in preventing diffusion of Rhodamine B dye into the PDMS by coating the surface with nanometer-sized SiO_2 particles; however, adsorption at the walls was still prevalent.²³ In a different method, sodium dodecyl sulfate was added to the fluid containing Rhodamine B and successfully prevented absorption; however, this modifies the working fluid and results in a significantly increased ζ potential.²⁵ Another suggested remedy is to coat the PDMS walls with a Polybrene solution.²¹ The positively charged Polybrene solution readily adsorbs onto the channel walls creating a barrier that repels Rhodamine B. In this study, various concentrations of Polybrene solution (10, 25, 50% w/v) were applied to a straight PDMS microchannel (150 $\mu\text{m} \times 100 \mu\text{m}$) before introducing a Rhodamine B solution. The results indicate that higher concentrations of Polybrene tend to reduce absorption but do not entirely eliminate the problem, prompting the search for a new method to alleviate Rhodamine B absorption.

Electrophoresis. The charge on a particle is dependent on such things as the surface chemistry and pH of the surrounding solution. Charged particles tend to migrate under an electric field. Positively charged particles (and to a lesser extent Rhodamine B) will migrate toward the cathode, and in the case of electroos-

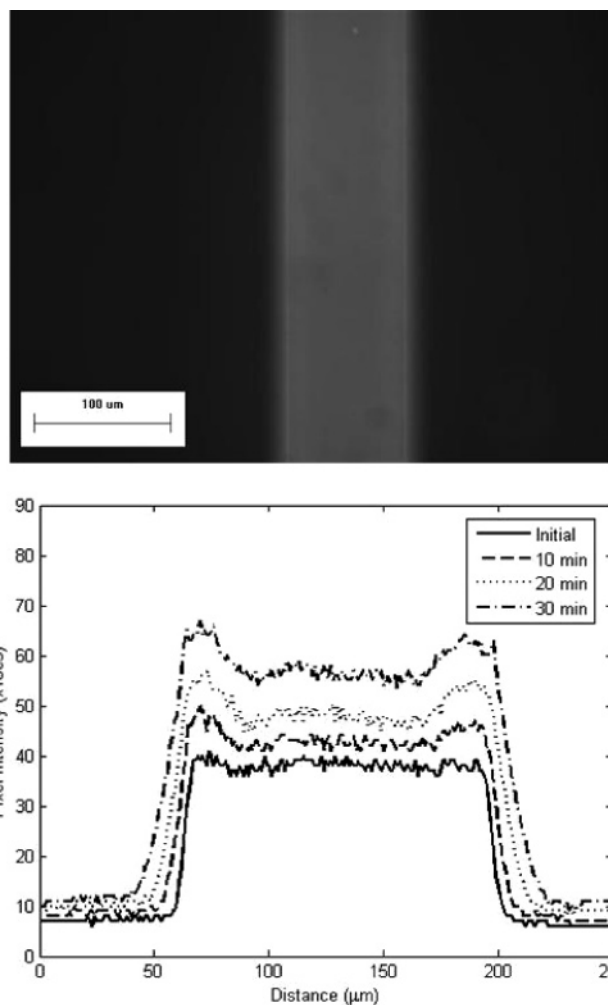


Figure 1. Image of a 100 μM Rhodamine B-filled PDMS microchannel after 30 min and the corresponding fluorescent intensity profile at 10, 20, and 30 min. Absorption and adsorption is evident due to the detectable fluorescent intensity extending beyond the channel walls and the peak intensities occurring at the solid–liquid interface.

motric pumping, electrophoresis of any charged fluorescent dyes is unavoidable. This results in an intensity gradient that will affect temperature measurements when electric fields are used.

Photobleaching. Photobleaching is a process in which fluorescent particles such as Rhodamine B dye, when subjected to excitation energies, undergo a chemical reaction in the fluorophore that prevents further fluorescent emissions.^{26,27} Photobleaching reduces fluorescent intensity over a very short time period making it difficult to take accurate temperature measurements. The photobleaching rate greatly depends on the photon flux and temperature, where higher temperatures correspond to greater photobleaching. It is an unavoidable phenomenon that can only be controlled by limiting the exposure dose or optimizing the concentration of the dye so that higher signals can be collected at lower doses.

Proposal of the New Method. As discussed above, the absorption and electrophoresis problems arise because Rhodamine B is mixed with the working fluid. In order to solve these two

(19) Xuan, X.; Xu, B.; Sinton, D.; Li, D. *Lab Chip* **2004**, *4*, 230–236.

(20) Erickson, D.; Sinton, D.; Li, D. *Lab Chip* **2003**, *3*, 141–149.

(21) Erickson, D.; Liu, X.; Venditti, R.; Li, D.; Krull, U. J. *Anal. Chem.* **2005**, *77*, 4000–4007.

(22) Ross, D.; Locascio, L. E. *Anal. Chem.* **2003**, *75*, 1218–1220.

(23) Roman, G. T.; Hlaus, T.; Bass, K. J.; Seelhammer, T. G.; Culbertson, C. T. *Anal. Chem.* **2005**, *77*, 1414–1422.

(24) Pittman, J. L.; Henry, C. S.; Gilman, S. D. *Anal. Chem.* **2003**, *75*, 361–370.

(25) Roman, G. T.; McDaniel, K.; Culbertson, C. T. *Analyst* **2006**, *131*, 194–201.

(26) Stinton, D. *Microfluid. Nanofluid.* **2004**, *1*, 2–21.

(27) Mosier, B. P.; Molho, J. I.; Santiago, J. G. *Exp. Fluids* **2002**, *33*, 545–554.

problems, Rhodamine B must be separated from the fluid and PDMS channels while still allowing for reliable temperature measurements. A novel method is developed in which a thin PDMS film is intentionally saturated with Rhodamine B and sandwiched between two glass substrates. This three-layer package is bonded to the PDMS mold containing the microchannel. A thin glass substrate ($150\ \mu\text{m}$) separates the liquid channel from the Rhodamine B film preventing dye diffusion into the liquid, thus eliminating absorption and electrophoresis. By visualizing the fluorescent intensity distribution, the temperature of the thin film can be obtained, providing a temperature estimate of the adjacent fluid channel. Although the liquid temperature is not measured directly, the error in predicting the liquid temperature can be limited by properly controlling the heat transfer of the system, which will be discussed later. The current design may not provide a very high degree of accuracy due to the thickness of the film and glass substrate ($\sim 180\ \mu\text{m}$ in total); however, it is a simple and cost-effective method for resolving Rhodamine B and PDMS compatibility issues and serving as a design tool for chip prototyping and characterization. An additional advantage is that whole-chip temperature field can be measured, whereas with the conventional method only the liquid temperature in the microchannel can be measured. This allows for the study of temperature gradients and subsequent heat transfer throughout the chip.

EXPERIMENTAL METHOD AND MATERIALS

Fabrication of PDMS Thin Film with Rhodamine B. The use of thin polymer films doped with Rhodamine B for temperature measurement is not an entirely new concept. Romano et al.²⁸ studied the temperature measurement performance of Rhodamine B doped into a thin polymer film (Desmophen 651/Desmodur 75. Rhodamine B in proportions of 5:3:1). However, to the best of our knowledge, the doping of Rhodamine B into thin PDMS films for microfluidic temperature measurement applications has not been investigated. Two methods for thin-film fabrication using conventional soft lithography technology were considered. The first method involves mixing Rhodamine B with PDMS prepolymer prior to spin-coating onto a substrate to form the thin film. This option would provide exact control of the Rhodamine B concentration; however, Rhodamine B stains most surfaces, contaminating subsequent spin-coating processes. Also, during curing of the PDMS/Rhodamine B film, high temperatures may increase photobleaching and lower the overall fluorescent intensity. Therefore, to avoid the above-mentioned problems and to simplify the fabrication process, an immersion method was used with the following procedures.

A 1-mL aliquot PDMS (Dow Corning, Midland), in base-curing agent ratio of 10:1, is spun onto a microscope glass slide (VWR Intl., Mississauga, ON, Canada) at 3000 rpm for 60 s in a spin coater (Brewer Science Inc., Rolla, MO) to create a $30\text{-}\mu\text{m}$ layer and cured at $95\ ^\circ\text{C}$ for 3 min. Afterward, the substrate is submerged into a 5 mM solution (DI water) of laser grade Rhodamine B (Fisher Sci.) for 5 days and stored in the dark to ensure complete saturation of Rhodamine B. The substrate is then dried and plasma treated (Harrick Plasma, Ithaca, NY) with a

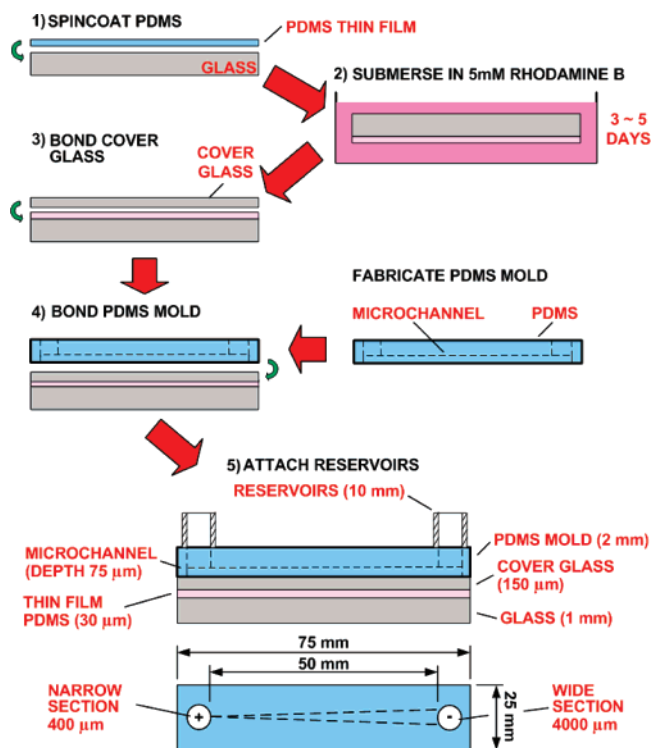


Figure 2. Schematic describing the fabrication process of the thin-film PDMS/Rhodamine B as well as the tapered microchannel device.

power of 29.6 W for 45 s. In preliminary designs, the PDMS/Rhodamine B film was directly bonded to the PDMS microchannel mold; however, the Rhodamine B particles would quickly diffuse back into the liquid and then into the walls of the PDMS mold. To prevent the backward diffusion of Rhodamine B, a $150\text{-}\mu\text{m}$ -thick cover glass slide (Brain Research Lab., Waban, ME) was plasma treated and bonded between the PDMS channel mold and the thin film as shown in Figure 2. The effects of the cover glass and thin-film thickness on temperature measurements is included in the Results and Discussion section. The film was stored in the dark when not in use to prevent photobleaching. Inadvertent photobleaching caused by ambient light restricts the thin-film method to being used as a design tool for prototyping and characterization.

Temperature Measurement Using PDMS/Rhodamine B Thin Film. The thin PDMS/Rhodamine B film (excitation, 500–550 nm; emission, $>565\ \text{nm}$) is excited by a 100-W halogen lamp light source through a neutral density filter with a 25% transmission to reduce the amount of photobleaching. A $5\times$ objective in an inverted microscope (GX-71, Olympus) along with a 1392×1040 pixel CoolSNAP ES Monochrome CCD camera with progressive scan (Photometrics, Tuscon, AZ) is used to record the images (exposure time 8 s). Each image is analyzed by selecting and averaging the intensity values in a 20×20 pixel (representing an area of $25 \times 25\ \mu\text{m}$). A room-temperature intensity image is initially taken and used to normalize a subsequent intensity image of the same area after heating. The temperature is found by substituting the normalized intensity into a calibration curve. All experiments were performed in the dark, and the lamp shutter was closed when images were not being taken to prevent unnecessary photobleaching.

(28) Romano, V.; Zweig, A. D.; Frenz, M.; Weber, H. P. *Appl. Phys. B* **1989**, *49*, 527–533.

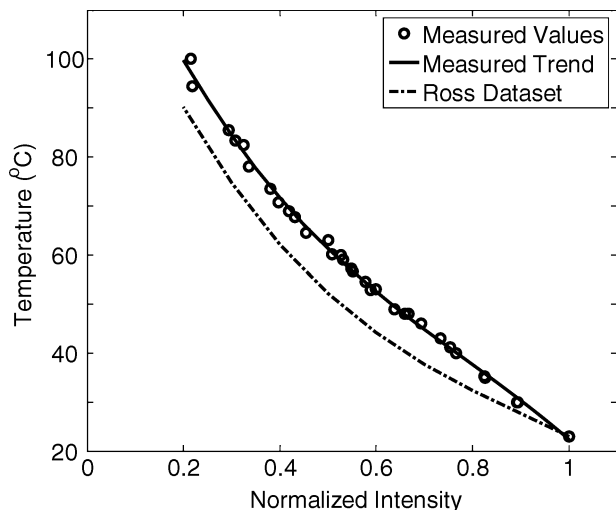


Figure 3. Calibration data for thin film including comparison with profile published by Ross et al.¹⁹

Calibration of PDMS/Rhodamine B Thin Film. The calibration procedure used in this study is adapted from experiments employed by Ross¹⁸ and Erickson²⁰ for conventional liquid-based Rhodamine B measurements. In brief, an intensity image of PDMS/Rhodamine B film is taken initially at room temperature and again after heating to a specific temperature. A thermocouple molded to the PDMS surface correlates the temperature with intensity. After imaging, the film is allowed to cool and a new baseline image is taken at room temperature before reheating so that photobleaching effects are not compounded. Recorded intensities are normalized with room-temperature intensity and plotted according to their temperatures to obtain a calibration curve. Since a calibration curve of thin PDMS/Rhodamine B film has never been reported, the calibration experiment was repeated for concentrations of 1 and 5 mM Rhodamine B solution dissolved into 30- μm -thick and 60- μm -thick thin films. These experiments show that Rhodamine B concentration and PDMS film thickness has no effect on the overall curve. The calibration curve is compared to results published by Ross¹⁸ as shown in Figure 3. The general trends of both calibrations are similar with larger discrepancies appearing at higher temperatures. Applying a third-order polynomial fit, the resulting temperature equation as a function of fluorescent intensity is

$$T = -96.904I^3 + 228.02I^2 - 250.25I + 141.53 \quad (1)$$

where I represents the normalized fluorescent intensity and T represents the temperature in Celsius degrees.

In terms of repeatability, the fluorescent intensity value of 10 thin films of PDMS/Rhodamine B was found to be similar, with an average value of 102.18 (at 23 °C) and a standard deviation of 1.59.

Application of PDMS/Rhodamine B Thin Film. The thin PDMS/Rhodamine B film was applied to measure the temperature distribution in a tapered PDMS microchannel subjected to an applied electrical field. Joule heating is unavoidably generated with nonuniform channel cross section resulting in an axial temperature gradient. Such a design has been applied to IEF applications,^{10,11,13} where the temperature gradient creates a pH gradient through a

pH-temperature-dependent buffer. For this study, a tapered microchannel silicon master with the dimensions of 75- μm depth, 50 mm long, 400 μm at the narrow end, and 4000 μm at the wide end was fabricated using standard soft lithography techniques.²⁻⁷ PDMS channel molds (base to curing agent ratio of 10:1) were cut and trimmed; fluid access holes were punched and the mold was irreversibly bonded via plasma treatment to the 150- μm glass side of the three-layer thin-film package. Glass reservoirs (1.5 cm high, 1/4-in. diameter, 3/8-in. outer diameter) were molded with PDMS over the top of the access holes to increase reservoir volume and reduce electrolysis effects. To prevent electroosmotic flow, 0.5% poly(vinylpyrrolidone) solution was flushed for 5 min before use and replaced with 25 mM Tris-HCl (pH 6.93, conductivity 1691 $\mu\text{S}/\text{cm}$), a commonly used buffer for IEF applications.

Room-temperature intensity images were initially taken along the channel at 5-mm intervals, and imaged again after 10 min of constant power supplied by a high-voltage sequencer (Labsmith HVS448, Labsmith, Livermore, CA), thus avoiding thermal runaway problems caused by electrolysis at the electrodes, which continually changes the electrical conductivity of the Tris-HCl.^{11,13} These images were then normalized, and the temperature was determined through the calibration curve.

Numerical Model. Numerical simulations of the temperature distribution in the tested chip were performed to corroborate the thin-film temperature experiments. The physical model for the temperature gradient generated in a tapered channel has been discussed thoroughly by others.^{11,29} Briefly, under an applied electric field, the fluid within the tapered channel experiences nonuniform internal heat generation in the form of Joule heating:

$$\dot{Q} = I^2/\sigma(T)A(x)^2 \quad (2)$$

where \dot{Q} represents the volumetric heat generation (W m^{-3}), I the current (A), A the area (m^2), and σ the electrical conductivity of the fluid (S m^{-1}). As shown in eq 2, Joule heating is dependent on the cross-sectional area, as a function of the axial location in the tapered channel. Therefore, the temperature will be a maximum at the narrow end and will gradually decrease toward the wide end of the channel. The temperature field at steady state can be described by the conservation of energy:

$$\rho c_p[\vec{u} \cdot \vec{\nabla} T] = \vec{\nabla} \cdot (k \vec{\nabla} T) + \sigma(T) \vec{E} \cdot \vec{E} \quad (3)$$

where ρ is the density (kg m^{-3}), c_p the specific heat ($\text{J kg}^{-1} \text{K}^{-1}$), k the thermal conductivity of the material ($\text{W m}^{-1} \text{K}^{-1}$), and \vec{u} the velocity vector (m s^{-1}). The effects of convection are assumed to be negligible since electroosmotic flow is suppressed. The electric field required as part of the internal heat generation is described by the following equations:

$$\nabla(\sigma \nabla \varphi) = 0 \quad (4)$$

$$\vec{E} = -\nabla \varphi \quad (5)$$

where φ is the electric potential (V). Most material properties remain relatively constant over the temperature range considered

(29) Kates, B.; Ren, C. L. *Electrophoresis* 2006, 27, 1967–1976.

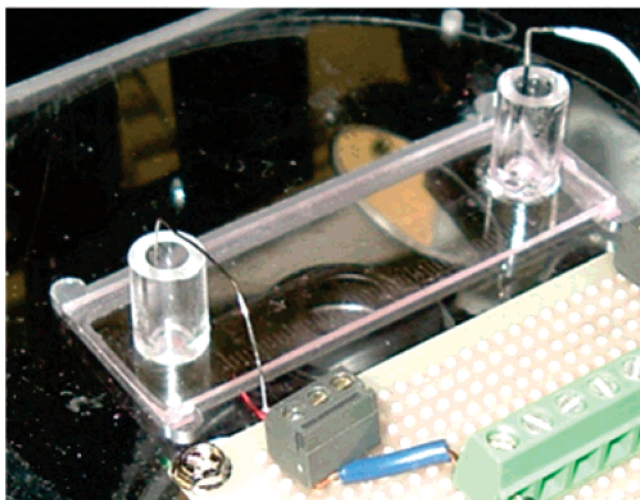
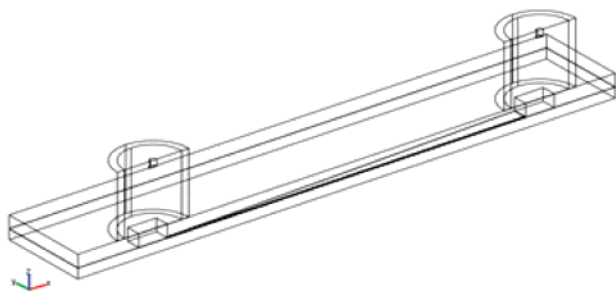


Figure 4. Setup of the inverted microscope for Rhodamine B intensity measurements and an enlarged schematic of the computational domain used in the numerical simulations.

in this study (25–80 °C) except for the electrical conductivity of the fluid, which is temperature dependent. The electrical conductivity of Tris-HCl versus temperature was measured and was expressed as $\sigma(T) = [1 + \alpha(T - T_0)]\sigma_0$, where α is the thermal coefficient (0.035 °C⁻¹) and σ_0 is the conductivity (1691 $\mu\text{S cm}^{-1}$) at the reference temperature T_0 (22.5 °C). Thermal properties of Tris-HCl were approximated as pure water and properties of the other materials were taken from the literature.^{20,30,31} The set of equations given above was solved for a 3-D model of the microfluidic chip using commercial finite element software (MULTIPHYSICS v3.3, COMSOL, Los Angeles, CA). The computational domain consists of a hybrid PDMS/glass microfluidic chip including a tapered channel and fluid reservoirs with platinum electrodes. To reduce the number of mesh elements, the thin PDMS/Rhodamine B film was replaced by a thermally equivalent thickness of glass (240 μm) through the equation, $k_{\text{PDMS}}/L_{\text{PDMS}} = k_{\text{glass}}/L_{\text{glass}}$. Due to symmetry, half of the geometry was chosen for the computational domain as shown in Figure 4.

For the electric field, insulation boundary conditions were placed along all outer surfaces and a constant power condition was applied through a voltage-dependent current flux ($I = P/V$, where P represents the applied power) at one electrode while the other was grounded. In the case of the thermal domain, an insulation condition was applied along the symmetry boundary.

As shown in Figure 4, the chip was placed in a custom-made acrylic holder that suspended the microfluidic chip over the inverted microscope objective. Consequently, there was decreased free air flow along the side walls of the chip and an insulation condition was applied. Natural convection heat-transfer coefficients were first computed from the Nusselt and Rayleigh numbers for the ideal case of a heated upper plate (top surface), heated lower plate (bottom surface), and heated side walls (reservoirs).³¹ In the first simulations, radiation effects were neglected; however, this resulted in a significant discrepancy between the numerical and experimental results. Therefore, a radiation heat-transfer coefficient was included in the boundary conditions, $h_{\text{rad}} = \epsilon\sigma(T_s + T_{\text{amb}})(T_s^2 + T_{\text{amb}}^2)$, where σ is the Stefan–Boltzmann constant and ϵ is the emissivity, which was assumed to be 0.9 for glass and PDMS.³¹ The heat-transfer coefficients were entered into the simulation as temperature-dependent functions since the radiation and natural convection heat transfer depends greatly on the local surface temperature. The coupled system of equations was solved simultaneously for 42 000 mesh elements using a nonlinear solver to determine the electric potential and temperature fields. The natural convection correlations assume a nearly uniform temperature distribution over the surface, which does not correspond with the local heating in the tapered channel. To account for this, the top and bottom heat-transfer coefficients were adjusted through the characteristic length in the Nusselt and Rayleigh numbers until the numerical results matched the experimental results for one case (400-mW input power). Afterward, all other numerical simulations were based off this characteristic length.

RESULTS AND DISCUSSION

Resolving Electrophoresis, Absorption, and Photobleaching. To verify that Rhodamine B did not diffuse into the channel mold, a thin PDMS/Rhodamine B film was reversibly bonded to the tapered channel. An electrical potential difference was applied to the tapered channel generating Joule heating (276 mW) in the liquid, heating up the liquid and surrounding material. The axial temperature gradient in the liquid resulted in temperature gradients in the thin PDMS/Rhodamine B film causing fluorescent intensity gradients in the thin film. After the fluorescent intensity was recorded along the channel, the PDMS channel mold was peeled off and checked for absorption where no Rhodamine B was found in the microchannel mold. Therefore, the cover glass successfully segregates the Rhodamine B dye from the working fluid and prevents any possible interference with the microchannel flow. This is also a proof of concept for preventing electrophoresis since the charged particles embedded inside the thin film will not be influenced by the electric fields passing through the working liquid.

Although this method cannot entirely eliminate photobleaching, its effect is significantly reduced by using a low-power halogen lamp as the excitation source combined with a neutral density filter and limiting the overall exposure time. To investigate this further, an experiment utilizing a tapered channel is devised in which three room-temperature intensity measurements were performed. First, the initial intensity at room temperature was recorded along the length of the tapered channel. Next, a constant power of 276 mW was applied for 10 min after which the thin film is subjected to halogen light excitation for 8 s. Subsequently, the microfluidic chip was cooled to room temperature and intensity

(30) Lide, D. R., Ed. *CRC Handbook of Chemistry and Physics*, 79th ed.; CRC Press: Boca Raton, FL, 1998.

(31) Incropera, F. P.; DeWitt, D. P. *Fundamentals of Heat and Mass Transfer*, 5th ed.; John Wiley and Sons: New York, 2002.

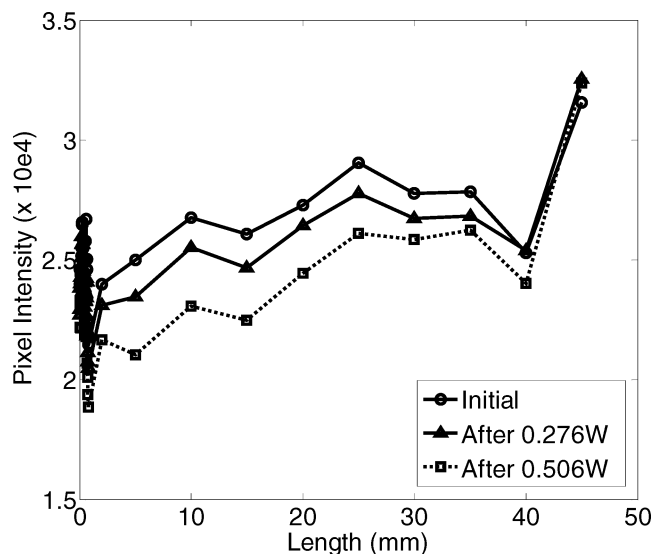


Figure 5. Change in room-temperature intensity readings due to photobleaching. An initial measurement is taken along the axis of the chip, and subsequent measurements are taken after a cycle of Joule heating where the chip is allowed to cool to room temperature.

measurements were taken. This process is repeated for a constant power of 506 mW. As shown in Figure 5, after each subsequent heating and exposure to halogen light, the room-temperature intensity in the whole channel decreases. Since diffusion has been prevented in the chip, any discrepancies in the intensity are solely due to photobleaching. However, intensity reduction differs along the axial length of the channel, with $\sim 8\%$ reduction near the narrow end, which decreases to 0.1% at the wide end. As this pattern corresponds to the heat generation and temperature distribution along a tapered channel, it can be surmised that higher temperatures increase the amount of photobleaching.

For repeated exposure doses, photobleaching will compound and reduce the baseline intensity, creating an error when compared to the initial image. Thus, after each use, the thin film should be brought to room temperature to establish a new baseline for normalizing the next temperature measurement. Compensating for the photobleaching without taking a new baseline image is difficult since it requires knowledge of the exposure conditions (dose, geometry, etc.) and the temperature of the film. However, it must be addressed that this problem is not specific to the thin film; the same effect should be observed in Rhodamine B-filled microchannels if there is not a constantly replenishing fluorescent dye source from fluid flow.

Tapered Channel Temperature Measurement and Validation. As previously discussed, the narrow region of the tapered channel has a larger electrical resistance, which results in greater local heating and higher temperatures. Axial temperature distributions obtained from thin-film experiments and numerical simulations for the tapered channel under 205-, 310-, and 400-mW conditions are shown in Figure 6. Each experimental curve represents the average temperature from two experiments performed with different chips of the same geometry. The location of the peak temperature for all powers remained relatively constant at 2.5 mm from the inlet, with a value of 39, 46, and 53 °C for 205, 310, and 400 mW, respectively. However, the peak temperatures are slightly higher than those predicted through simulations, with

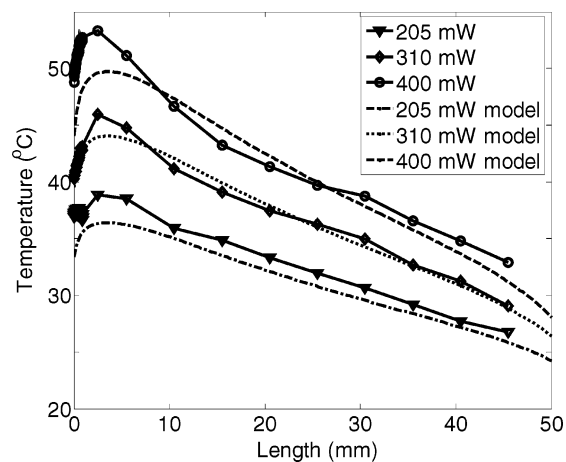


Figure 6. Experimental and numerical temperature profiles along the channel axis for constant powers of 205, 310, and 400 mW.

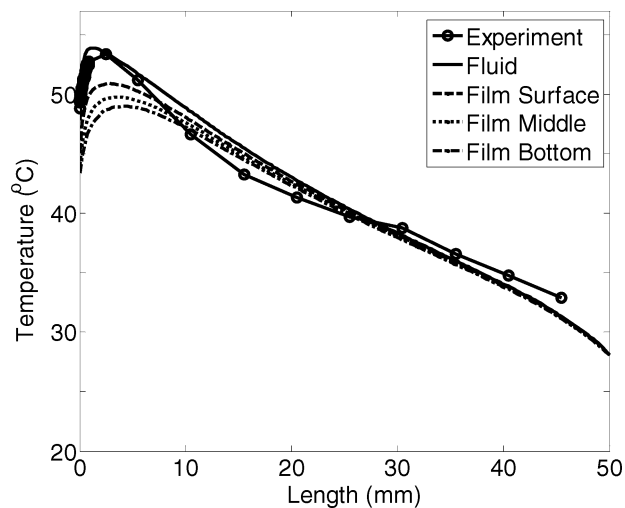


Figure 7. Comparison of the experimental temperature profile along the tapered channel for 400 mW to the results from the numerical model. Also included are the numerical temperature profiles at the top, middle, and bottom of the PDMS thin-film.

a value of 37, 43, and 49 °C, possibly due some geometric inconsistencies between the actual tapered channel and the one used in the numerical simulation. The peaks also represent locations with the largest discrepancy for each power setting, with at most 4 °C. The midfilm temperature from the numerical simulations and the experimental results follows similar temperature distribution trends along the length of the channel. In addition, validation using the traditional in-channel Rhodamine B injection method was attempted, with corresponding results and problems discussed in Appendix A (Supporting Information).

Figure 7 shows the numerically predicted temperature profile throughout the fluid and thin-film thickness as compared to the measured temperature for 400-mW input power, while Figure 8 provides a bright-field image overlaid with a temperature contour map of a tapered channel section. From the numerical results, one can see heat loss through the film results in a measured temperature (midfilm) slightly lower than the fluid temperature where the difference is largest at the peak temperature (3.5 °C difference midfilm to fluid). Through the film, the temperature difference is at most 2 °C at the peak location. Thermal diffusion also causes the sharp temperature peak in the fluid to be

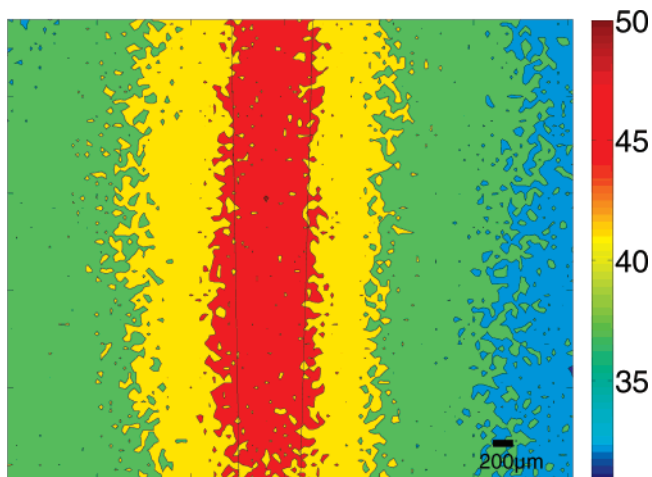


Figure 8. Temperature contour map overlaid with tapered channel layout at ~ 5 mm from the inlet. Heating effects diffuse into the surrounding side walls and are detected via Rhodamine B thin film.

smoothed out at the thin-film plane. The low-temperature variation through the film can be attributed to the specific heat transfer of the system. It implies that the experimentally measured temperature using the thin-film method generally underpredicts the liquid temperature. Modeling the thin film in a parallel plate limit as a two-layer composite geometry, the estimated time constant of the film to a step change in temperature at the microchannel is 112 ms.³² Therefore, one can estimate the thermal time response of the thin film to be on the order of a few seconds (2–4 s).

An additional advantage of the thin Rhodamine B film is that the side walls surrounding the channels can be detected, providing more temperature distribution information compared to traditional fluid-based fluorescent dye methods. Heating effects generally diffuse into the surrounding side walls of the channel due to low heat conduction. Applying a simple 1-D thermal resistance analysis to the bottom (thin film and glass) and top of the chip (PDMS mold), the total thermal resistance is a combination of the conduction and convection/radiation resistances:³¹

$$R_{\text{Top}} \propto \frac{1}{h_t} + \frac{L_{\text{PDMS}}}{k_{\text{PDMS}}}$$

$$R_{\text{Bottom}} \propto \frac{1}{h_b} + \frac{L_{\text{film}}}{k_{\text{PDMS}}} + \frac{L_{\text{glass}}}{k_{\text{glass}}} \quad (6)$$

where h is the total heat-transfer coefficient (convection and radiation) of the surface, k the thermal conductivity, and L is the layer thickness. Equation 6 allows for order of magnitude estimates of how the chip design affects the heat transfer of the system. The calculations show that the convection and radiation resistance is 2 orders of magnitude higher than the conduction resistance for the bottom layer ($R_{\text{conv}}/R_{\text{cond}} \approx 100$) and 1 order of magnitude higher through the top ($R_{\text{conv}}/R_{\text{cond}} \approx 6$). Thus, heat transfer is dominated by convection and radiation resistance, which explains the low-temperature variations through the film.

(32) Absi, J.; Smith D. S.; Nait-Ali, B.; Grandjean, S.; Berjonnaus, J. J. *Eur. Ceram. Soc.* **2005**, *25*, 367–373.

In addition, heat transfer through the top and bottom are nearly equivalent ($R_{\text{Top}}/R_{\text{Bottom}} \approx 0.85$).

The low-temperature variation through the film is also a result of suspending the microfluidic chip over the inverted microscope during the experiments. However, if the chip was placed on a large flat surface, as is the case when an upright microscope is used, heat transfer would occur mainly through the bottom surface and temperature variations through the film will be significant. An estimate shows the temperature difference between the fluid and the thin film could be as high as 25–40%, which implies that the thin-film method cannot be used to measure the liquid temperature in such a scenario. Due to these discrepancies in heat transfer, actual fluid temperature measurements are not possible; rather, the thin-film method provides a close approximation of the in-channel temperatures. To accurately measure the fluid temperature the film must be placed closer to the microchannel and the thermal resistance of the film must be reduced by decreasing its thickness. This may be accomplished by spin coating an ultrathin layer ($< 5 \mu\text{m}$) of PDMS and replacing the cover glass with another thin layer of material impermeable to Rhodamine B.

CONCLUSION AND RECOMMENDATIONS

A new method of performing on-chip temperature measurement using thin PDMS film embedded with Rhodamine B dye has been presented. The thin fluorescent PDMS film resolves the compatibility issues of using Rhodamine B dye to measure temperature distributions in PDMS microchannels. Rhodamine B dye is successfully segregated from the fluid channel, thus preventing diffusion and any possible electrophoresis of the charged dye particles. Although this method of temperature measurement does not eliminate photobleaching, it is reduced by using a much lower excitation source. The film was applied to measure the temperature field in a tapered microchannel subjected to Joule heating, and results compared well with numerical simulation results. The thin PDMS/Rhodamine B film provides long-term temperature measurement without directly interfering with the channel and working liquid. In addition, the thin film allows for whole-chip temperature measurements at the thin-film plane. Due to the high thickness of the thin film, its current application is limited to cases where there is little temperature variation through the film thickness. Future work will entail developing a thinner film to reduce measurement errors and to measure temperature profiles in devices for isoelectric focusing with thermally generated pH gradients.

ACKNOWLEDGMENT

The authors gratefully acknowledge the support of a Research Grant of the Natural Sciences and Engineering Research Council (NSERC) of Canada to C.R. and Canada Graduate Scholarship to T.G.

SUPPORTING INFORMATION AVAILABLE

Additional information as noted in text. This material is available free of charge via the Internet at <http://pubs.acs.org>.

Received for review June 16, 2007. Accepted October 22, 2007.

AC071268C